

Crystalline ground states of an entropically stabilized quasicrystal model

H. K. Lee,* R. H. Swendsen, and M. Widom

Department of Physics, Carnegie Mellon University, Pittsburgh, Pennsylvania 15213

(Received 5 July 2001; published 19 November 2001)

A binary Lennard-Jones alloy exhibits an entropically stabilized quasicrystal state in two dimensions at elevated temperatures. We consider the ground states of this model by calculating the convex hull of cohesive energy as a function of alloy composition. Only crystalline structures with rational values of the composition appear on vertices of the convex hull. In particular, at the irrational composition of the ideal quasicrystal structure, the ground state is a coexisting mixture of two nearby quasicrystal approximants.

DOI: 10.1103/PhysRevB.64.224201

PACS number(s): 61.50.-f, 64.70.Pf

I. INTRODUCTION

A binary Lennard-Jones alloy in two dimensions was the first atomistic model of a decagonal quasicrystal.^{1,2} Monte Carlo simulations of this model² found that thermodynamically stable decagonal quasicrystals form spontaneously from the disordered liquid state as the temperature drops. Later molecular dynamics simulations³ confirmed this finding. Besides being used in quasicrystal studies⁴⁻⁹ the model has been used to study viscoplastic deformation¹⁰ in amorphous solids and used for comparison between multicanonical methods, molecular dynamics, and Monte Carlo methods.¹¹

Despite much effort put into the study of quasicrystals, some fundamental questions about quasicrystals have not been answered completely. One essential issue is the mechanism by which quasicrystals become thermodynamically stable. This question is best considered in the context of tilings of space by rigid geometrical tiles decorated with atoms. Levine and Steinhardt¹² proposed that quasicrystals are stabilized by tile matching rules that force quasiperiodicity in the ground state. Elser¹³ and Henley¹⁴ pointed out that random tilings spontaneously form quasicrystals without the need for matching rules. It was then proposed by Widom^{2,15} that certain quasicrystals are stabilized by the configurational entropy of their phason fluctuations. In this scenario, quasicrystal-forming compounds exhibit conventional crystalline states at low temperatures, then transform into the quasicrystal at intermediate temperatures before melting at higher temperatures yet. The phason elastic constants should exhibit a linear temperature dependence due to their entropic origin.^{7,14}

Skibinsky *et al.*¹⁶ showed that quasicrystal states with a square well potential are indeed entropically stabilized, though here the free volume entropy also plays a role. On the contrary, Miekisz¹⁷ constructed finite-range lattice gas models that have stable quasicrystalline ground states, and Jagla¹⁸ found stable quasicrystalline ground states using a repulsive potential.

Evidence abounds that the quasicrystal state of the binary Lennard-Jones alloy is stabilized at finite temperatures by configurational entropy. Among the evidence: observation of phason flips in Monte Carlo and molecular dynamics simulations;^{2,3} calculation of entropy and phason elastic constants arising from the ground-state degeneracy when inter-

actions are truncated at near neighbors;⁴ calculation of phason elastic constant proportional to temperature;^{5,7} and observation of a low-temperature instability of the quasicrystal phase.⁷ Despite this evidence of entropic stabilization of the quasicrystal state, confirmation of the crystallinity at low temperatures has remained elusive. Our present work investigates the ground states of this model and confirms their crystalline nature.

II. THE MODEL FOR QUASICRYSTAL STATE

We used the binary Lennard-Jones alloy model introduced by Lancon, Billard, and Chaudhari¹ and independently by Widom, Strandburg, and Swendsen.² This model consists of large and small particles, denoted by L and S , respectively. Interaction energies favor mixing of unlike particle types. Optimal bond lengths encourage ten small particles to surround a large particle and five large particles to surround a small particle, hence favoring tenfold symmetry in the quasicrystal. Mathematically, the interaction potentials between particles of types α and β are

$$V_{\alpha\beta}(r) = E_{\alpha\beta}[(\sigma_{\alpha\beta}/r)^{12} - (\sigma_{\alpha\beta}/r)^6], \quad (1)$$

where the interaction energies are $E_{LS} = 1$, $E_{LL} = E_{SS} = 1/2$ and the optimal bond lengths are $\sigma_{LS} = 1$, $\sigma_{LL} = 2 \sin 36^\circ$, $\sigma_{SS} = 2 \sin 18^\circ$. The total energy of a configuration of N particles is

$$E_{\text{tot}} = \frac{1}{2} \sum_{i \neq j=1}^N V_{\alpha(i)\beta(j)}(r_{ij}) \quad (2)$$

with $\alpha(i)$ and $\beta(j)$ indicating the types of particles i and j . We use the units $T^* = k_B T / E_{LS}$ and $U^* = E_{\text{tot}} / E_{LS}$. We denote the numbers of large and small particles N_L and N_S , and define the composition variable

$$x \equiv \frac{N_S}{N_S + N_L}. \quad (3)$$

Our goal is to determine the ground state structure as a function of x .

Low energy configurations of this model cover the plane with tile structures (see Fig. 1). We may describe these tilings using a primitive set of “thin” 36° and “fat” 72° rhombus tiles known as “binary tiles.”^{3,4} The numbers of small

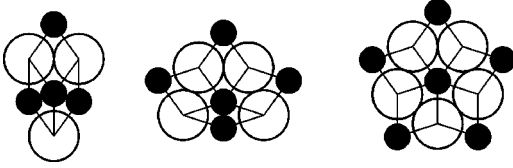


FIG. 1. Fat and thin binary rhombus tiles decorated with large and small particles. Rhombi combine to form hexagon, boat, and star tiles.

and large particles relate to the numbers of thin and fat rhombi (N_T and N_F) through the linear equation

$$\begin{pmatrix} N_L \\ N_S \end{pmatrix} = \begin{pmatrix} 3/5 & 1/5 \\ 2/5 & 4/5 \end{pmatrix} \begin{pmatrix} N_F \\ N_T \end{pmatrix}. \quad (4)$$

Since fat and thin tiles occur in the ratio of $\tau:1$ in a structure with tenfold symmetry, Eq. (4) determines the ideal quasicrystal composition

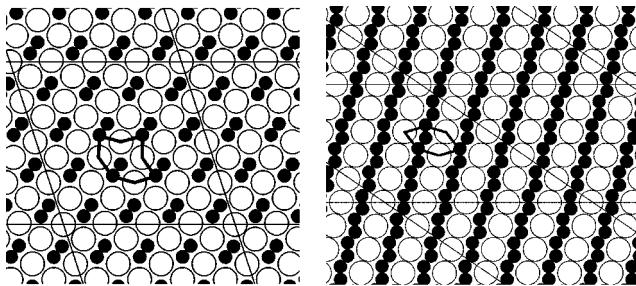
$$x_Q = \frac{2}{\tau+2} = 0.552786\dots, \quad (5)$$

where $\tau = (\sqrt{5}+1)/2 = 1.61803\dots$ is the golden mean.

Alternatively, we may take certain groups of binary tiles that form larger “hexagon,” “boat,” and “star” tiles (see Fig. 1). Every binary rhombus tiling may be reexpressed as a hexagon-boat-star tiling. The hexagonal tile contains one large and two small particles and is formed by putting together one fat rhombus and two thin rhombi. The boat tile contains two large and two small particles and is formed by putting together three fat rhombi and one thin rhombus. The star tile contains three large and two small particles and is formed by putting together five fat rhombi. The linear relationship between the number of large and small particles and the number of hexagon, boat, and star tiles is

$$\begin{pmatrix} N_L \\ N_S \end{pmatrix} = \begin{pmatrix} 1 & 2 & 3 \\ 2 & 2 & 2 \end{pmatrix} \begin{pmatrix} N_{\text{hex}} \\ N_{\text{boat}} \\ N_{\text{star}} \end{pmatrix}. \quad (6)$$

In particular, the composition of a pure boat tiling is $x_B = 1/2$ and the composition of a pure hexagon tiling (see Fig. 2) is $x_H = 2/3$. Pure star tilings do not exist. Because Eq. (6)



$X=1/2 = 0.500000$ [B]

$X=2/3 = 0.666\dots$ [H]

FIG. 2. Configurations that forms the convex hull, unit cells form with boat tiles [B] and hexagonal tiles [H] are drawn in bold lines.

is not invertable, there exists no fixed ratio of $N_{\text{hex}}:N_{\text{boat}}:N_{\text{star}}$ at the quasicrystal composition X_Q .

This model exhibits a highly degenerate ground state when the potentials are truncated at nearest neighbors.^{2,4} The degeneracy is given by the number of distinct ways to tile the plane with hexagons, boats, and stars. Consequently, the true ground state depends sensitively on how we treat the long-range tail of the potential. For this paper we address the full, untruncated, Lennard-Jones interaction defined in Eq. (1), and all of our reported ground-state energies are calculated in this manner. In order to evaluate the energies numerically, we carry the summation in Eq. (2) explicitly out to sufficiently large r that the energy per particle E_{tot}/N converges to 10^{-7} .

To study the model at low temperatures, we calculated the energy of many structures at a large number of compositions around the quasicrystal composition. The convex hull¹⁹ of a plot of energy per particle versus composition aids in determination of the composition-dependent ground state. Suppose (x_1, E_1) and (x_2, E_2) are consecutive vertices of the convex hull with $x_1 < x_2$. Then the ground state energy of a structure of composition x between x_1 and x_2 is given by the tie line

$$E(x) = E_1 + \frac{E_2 - E_1}{x_2 - x_1}(x - x_1). \quad (7)$$

Typically this energy will be achieved by phase separation of the N particles into a region of space containing

$$N_1 = \frac{x_2 - x}{x_2 - x_1}N, \quad (8)$$

$$N_2 = \frac{x - x_1}{x_2 - x_1}N \quad (9)$$

particles of phase 1 and phase 2, respectively. For finite N , Eq. (7) serves as a lower bound on the energy. Generally the interface between the two phases raises the total energy above the tie line. As $N \rightarrow \infty$, the interfacial energy cost *per particle* vanishes.

III. MONTE CARLO SIMULATION AND ENERGY MINIMIZATION

To find the ground-state energies, we confined our particles to a parallelogram with periodic boundary conditions in thermal equilibrium with an empty box and performed Monte Carlo simulations.²⁰ In addition to simulating the individual particles' continuous motion in space using the Metropolis algorithm, our Monte Carlo moves allowed for three particle flip moves,² changes in the box volumes while keeping the sum of the volumes of boxes constant, and changes in the angle and aspect ratio of the periodic boundary conditions. The empty box maintains zero pressure for our simulation. In principle, systems at nonzero temperature will eventually evaporate at zero pressure. Our simulations did not show evaporation, partially because of the finite total volume. That is, the pressure is exceedingly low but not truly zero.

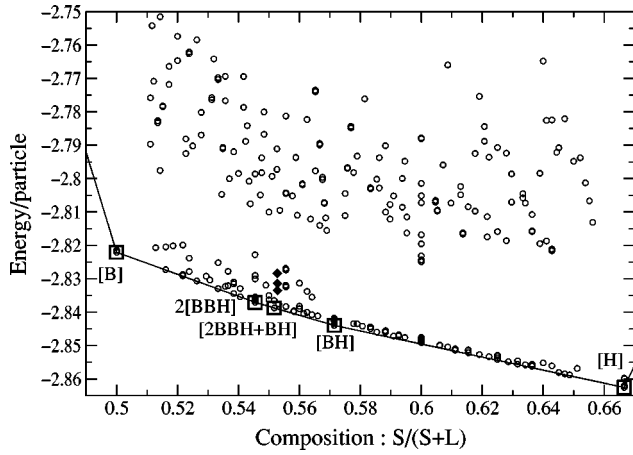


FIG. 3. Plot of energy per particle versus particle composition. Squares show the points on the convex hull and diamonds show low-energy configurations of a quasicrystal approximant at composition x_A . Bands of high-energy points originated from configurations that have vacancies or substitutional defects.

We systematically performed simulations at all compositions x containing $N \leq 45$ particles per cell over the composition range $x_B = 0.5 \leq x \leq x_H = 0.666 \dots$. For compositions in the range $0.53061 \leq x \leq 0.5689$ we did additional simulations at all compositions containing $N \leq 65$ particles. At every composition, 80–200 low-energy configurations were relaxed using conjugate gradient minimization. For finite temperature Monte Carlo simulations we truncate the potential at $4\sigma_{LL}$ for the sake of computational efficiency. However, the full long range interaction was included in all subsequent conjugate gradient relaxations. Conjugate gradient minimizations ran until energies converged to 5×10^{-5} .

In addition to systematically searching for low-energy configurations using simulations, we constructed several candidate low-energy configurations by hand, then used conjugate gradient minimization to find low-energy states close to these configurations.

The freezing temperature for our system is between $T^* = 0.3$ and 0.18 . We did simulations of 55 000 MCS/P (MCS/P means Monte Carlo steps *per particle*) starting from the liquid state and cooling from $T^* = 0.3$ to 0.18 , followed by 30 000 MCS/P cooling from $T^* = 0.18$ to 0.08 and 15 000 MCS/P cooling from $T^* = 0.08$ to 0.01 . An annealing scheme was determined dynamically by requiring that the energy histograms overlap to within $1/n$ standard deviations, n represents the degree of annealing. We set $n=2$ between $T^* = 0.3$ and 0.18 , $n=3$ between $T^* = 0.18$ and 0.08 , and $n=1$ between $T^* = 0.08$ and 0.01 . All configurations of a given N and composition are obtained from a single cooling run. However, there are many different low-energy configurations for each single run due to the phason flips.

IV. RESULTS

We found over a hundred low-energy configurations (within an energy of about 0.1 of the tie-line energy), which are plotted in an energy-composition plot in Figs. 3 and 4. By comparing these energy states, we could identify the

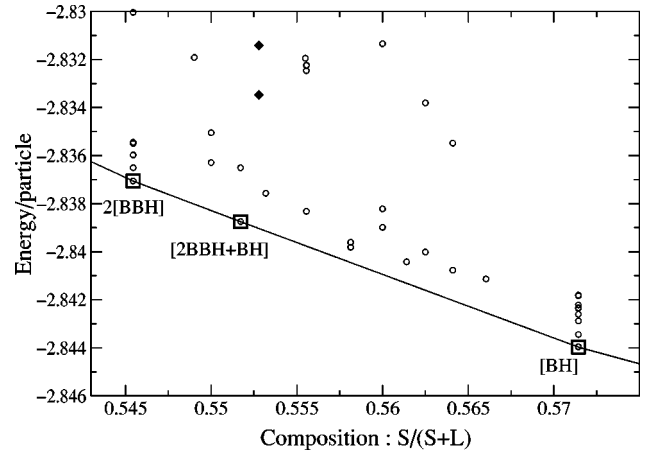


FIG. 4. Plot showing details of low-energy compositions near the quasicrystal composition.

stable crystalline states from the convex hull of the energy-composition plot. There is a band of relatively high-energy configurations in Fig. 3. These are configurations with vacancies or substitutional defects, and hence are not tilings of the plane by decorated binary tiles.

Crystalline configurations that form the convex hull are shown in Figs. 2 and 5. The simplest configurations forming the convex hull are those with one boat tile [B] ($x_B = 1/2$) or one hexagonal tile [H] ($x_H = 2/3$) as the unit cell (see Fig. 2). The remaining configurations that lie on the convex hull are shown in Fig. 5. Equal proportions of boat tiles and hexagonal tiles can be mixed to obtain the [BH] structure at composition $x_{BH} = 4/7 = 0.571428$. Mixing two [BH] unit cells and two B unit cells produces another point on the convex hull with a unit cell of [2(BBH)] at composition $x_{2[BBH]} = 6/11 = 0.545454 \dots$. It seems that there is no way to tile the plane with just a single [BBH] per unit cell, hence the

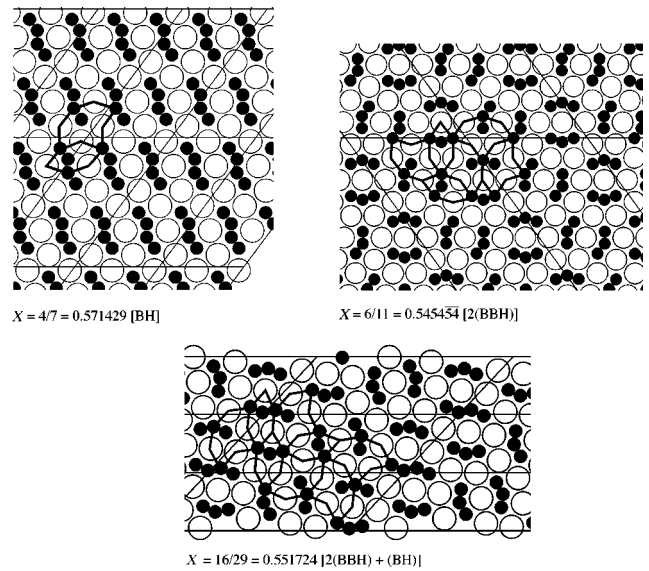


FIG. 5. Configurations that form the convex hull, unit cells that form with boat tiles [B] and hexagonal tiles [H], are drawn in bold lines.

need to double the cell. The last point on the convex hull mixes the [2(BBH)] unit cell with the [BH] unit cell to create [2(BBH)(BH)] at composition $x = 16/29 = 0.551724 \dots$, which is rather close to the quasicrystal composition ($x_Q = 0.55278 \dots$).

Let us point out several compositions that do not appear on the convex hull. We considered the mixtures [(BBH)(BH)] and [2(BBH)2(BH)], both at $x = 5/9 = 0.5555 \dots$, but were unable to find any structure on the convex hull. We also considered [(H)(BH)], [2(BBH)2(B)] and [2(BBH)(B)], again failing to find any structure on the convex hull.

Of special note is the effort we made very close to the ideal quasicrystal composition. We used a unit cell of 152 particles containing 84 small particles and 68 large particles to approximate the quasicrystal state. The composition of this special quasicrystal approximant unit cell is $x_A = 84/152 = 0.552632$, which is just slightly less than the ideal quasicrystal composition given in Eq. (5). We did three independent simulations to anneal this quasicrystal approximant. As before, 80–200 states (from each run) were used as the input for conjugate gradient minimizations. The lowest energy configuration found in each of these three runs is plotted on Figs. 3 and 4.

The lowest energy configurations we identified at this composition are shown as black diamonds in the convex hull plots. These configurations all tile the plane with 16 hexagons and 26 boats. The lowest energy found lies about $\Delta E = 0.005$ per particle above the tie line. Given the entropy per particle $S = 0.193$ available from phason fluctuations,⁴ we can estimate that this approximant could be entropically stabilized above temperature $T = \Delta E/S = 0.026$. Assuming these values are representative of the ideal quasicrystal composition, we obtain a rough estimate of the temperature at which

a crystal to quasicrystal transition might occur in our model.

Crystals containing star tiles (S) are conspicuously missing from the convex hull. It appears that points on the convex hull contain only B and H tiles. Some of the structures lying above the convex hull do contain star tiles but these can be considered as grain boundary defects between star-free crystalline domains.

V. CONCLUSIONS

According to the convex hull, at composition x_Q the ground state of an infinite system is a pair of coexisting crystal phases. The system should phase separate into a crystalline domain [2(BBH)(BH)] and a crystalline domain of [BH]. Because [2(BBH)(BH)] is so much closer in composition to the ideal quasicrystal than [BH] is, the largest fraction of particles

$$\frac{N_{[2(BBH)(BH)]}}{N} = \frac{x_{[BH]} - x_Q}{x_{[BH]} - x_{[2(BBH)(BH)]}} = 0.946 \quad (10)$$

will form the phase [2(BBH)(BH)]. Since the true ground state is crystalline, the thermodynamically stable quasicrystal state in the binary Lennard-Jones alloy must be stabilized by entropy. Now that the ground state has been identified, it will be possible to examine the transition from the crystalline ground state into the high-temperature quasicrystal state through further computer simulations.

ACKNOWLEDGMENTS

We would like to thank M. Mihalkovic and E. Cockayne for constructive discussions and assistance. This work was supported in part by the NSF under Grant No. DMR-9732567.

*Present address: Dept. of Physics and Astronomy, University of Georgia, Athens, GA 30602.

¹F. Lancon, L. Billard, and P. Chaudhari, *Europhys. Lett.* **2**, 625 (1986).

²M. Widom, K.J. Strandburg, and R.H. Swendsen, *Phys. Rev. Lett.* **58**, 706 (1987).

³F. Lancon and L. Billard, *J. Phys. (France)* **49**, 249 (1988).

⁴M. Widom, D.P. Deng, and C.L. Henley, *Phys. Rev. Lett.* **63**, 310 (1989).

⁵K.J. Strandburg, L.-H. Tang, and M.V. Jaric, *Phys. Rev. Lett.* **63**, 314 (1989).

⁶K.J. Strandburg, *Phys. Rev. B* **40**, 6071 (1989); **44**, 4644 (1991).

⁷H.-C. Jeong and M. Widom (unpublished).

⁸R. Mikulla, J. Roth, and H.R. Trebin, *Philos. Mag. B* **71**, 981 (1995).

⁹J. Gazeau, R. Krejcar, and J. Miekisz, *Mater. Sci. Eng., A* **294-**

296, 421 (2000).

¹⁰M.L. Falk and J.S. Langer, *Phys. Rev. E* **57**, 7192 (1998).

¹¹K.K. Bhattacharya and J.P. Sethna, *Phys. Rev. E* **57**, 2553 (1998).

¹²D. Levine and P.J. Steinhardt, *Phys. Rev. Lett.* **53**, 2477 (1984).

¹³V. Elser, *Phys. Rev. Lett.* **54**, 1730 (1985).

¹⁴C. L. Henley, in *Quasicrystals: the State of the Art*, edited by D. P. Di Vincenzo and P. J. Steinhardt (World Scientific, Singapore, 1991), p. 429.

¹⁵M. Widom, in *Quasicrystals*, edited by M. V. Jaric and S. Lundqvist (World Scientific, Singapore, 1990), p. 337.

¹⁶A. Skibinsky, S.V. Buldyrev *et al.*, *Phys. Rev. E* **60**, 2664 (1999).

¹⁷J. Miekisz, *J. Stat. Phys.* **88**, 691 (1997).

¹⁸E.A. Jagla, *Phys. Rev. E* **58**, 1478 (1998).

¹⁹J. Hafner, *From Hamiltonians to Phase Diagrams* (Springer-Verlag, Berlin, 1987).

²⁰A.Z. Panagiotopoulos, *Mol. Phys.* **61**, 813 (1987).